Atmos. Chem. Phys. Discuss., https://doi.org/10.5194/acp-2018-935
Manuscript under review for journal Atmos. Chem. Phys.
Discussion started: 6 November 2018

Atmospheric Chemistry and Physics Discussions

Oligomerization Reactions of Criegee Intermediates with Hydroxyalkyl Hydroperoxides: Mechanism, Kinetics, and Structure-Reactivity Relationship

Long Chen, [1,2] Yu Huang, *[,1,2] Yonggang Xue, [1,2] Zhenxing Shen,[3] Junji Cao, *[,1,2] Wenliang Wang[4]

[1] *Key Lab of Aerosol Chemistry & Physics, Institute of Earth Environment, Chinese Academy of Sciences, Xi'an, Shaanxi, 710061, China*

[2] *State Key Laboratory of Loess and Quaternary Geology, Institute of Earth Environment, Chinese Academy of Sciences, Xi'an 710061, China*

[3] *Department of Environmental Sciences and Engineering, Xi'an Jiaotong University, Xi'an, 710049, China*

[4] *School of Chemistry and Chemical Engineering, Key Laboratory for Macromolecular Science of Shaanxi Province, Shaanxi Normal University, Xi'an, Shaanxi, 710119, China*

*Corresponding author:

Prof. Yu Huang, E-mail address: huangyu@ieecas.cn

Prof. Junji Cao, E-mail address: cao@loess.llqg.ac.cn

Atmos. Chem. Phys. Discuss., https://doi.org/10.5194/acp-2018-935
Manuscript under review for journal Atmos. Chem. Phys.
Discussion started: 6 November 2018

Atmospheric Chemistry and Physics Discussions

ABSTRACT:

Although secondary organic aerosols (SOAs) are major components of $PM_{2.5}$ and organic aerosol (OA) particles and therefore profoundly influencing air quality, climate forcing and human health, the mechanism of SOAs formation via Criegee chemistry is poorly understood. Herein, we perform high-level theoretical calculations to study the reactivity and kinetics of four Criegee intermediates (CIs) reactions with four hydroxyalkyl hydroperoxides (HHPs) for the first time. The calculated results show that the sequential addition of CIs to HHPs affords oligomers containing CIs as chain units. The addition of -OOH group in HHPs to the central carbon atom of CIs is identified as the most energetically favorable channel, with a barrier height strongly dependent on both, CI substituent number (one or two) and position (*syn*- or *anti*-). In particular, the introduction of a methyl group into the *anti*-position significantly increase the rate coefficient, dramatic decrease is observed when the methyl group is introduced into the *syn*-position. Based on the collected data, the atmospheric lifetime of *anti*-CH_3CHOO in the presence of HHPs is estimated as ~5.9×10^3 s. These findings are expected to broaden the reactivity profile and deepen our understanding of atmospheric SOAs formation processes.

Atmos. Chem. Phys. Discuss., https://doi.org/10.5194/acp-2018-935
Manuscript under review for journal Atmos. Chem. Phys.
Discussion started: 6 November 2018

Atmospheric Chemistry and Physics Discussions

1. Introduction

Alkenes are the most abundant volatile organic compounds (VOCs) in the atmosphere after methane and primarily originate from anthropogenic and biogenic sources (Lester et al., 2018). Gas-phase ozonolysis of volatile alkenes is extremely exothermic, and the potential energy surface (PES) following the 1,3-cycloaddition of ozone to the C=C double bond forming a primary ozonide (POZ) is riddled with shallow wells and low barriers (Donahue et al., 2011; Aplincourt et al., 2000), which then dissociate to produce a carbonyl oxide (also called Criegee intermediates (CIs)) and a carbonyl moiety (Johnson et al., 2008; Welz et al., 2012; Criegee, 1975). Alkene ozonolysis is thought to be an important source of radicals, whose subsequent reactions lead to the formation of hydroperoxides, organic peroxides, and secondary organic aerosols (SOAs) (Donahue et al., 2011; Becker et al., 1990; Kroll et al., 2008; Hallquist et al., 2009; Tobias et al., 2001), and thus influence air quality, climate forcing and human health (Rissanen et al., 2014; Donahue et al., 2011; 2012). Criegee intermediates were first proposed by Rudolph Criegee as early as 1975 (Criegee, 1975), and their direct synthesis in the laboratory experiment were performed by the photolysis of organic iodides in the presence of O_2 and the photolytic Cl-initiated oxidation of dimethyl sulfoxide (DMSO) (Welz et al., 2012; Taatjes et al., 2008).

In view of the highly exothermic nature of alkene ozonolysis, the nascent CIs often possess a considerable amount of internal energy and are thus highly reactive (Li et al., 2018; Li et al., 2014). The thermal unimolecular decay of vibrationally excited CIs is thought to be an important nonphotolytic source of atmospheric hydroxyl (OH) radicals, particularly in low light conditions, urban environments, and heavily forested areas (Lester et al., 2018; Foreman et al., 2016; Kidwell et al., 2016; Green et al., 2017; Zhang et al., 2002). OH radical is one of the most powerful oxidants that participates in the atmospheric photochemical oxidation of VOCs (Gligorovski et al., 2015), and thus contributes to tropospheric ozone formation by being involved in the production of organic peroxy radicals (RO_2), which, in turn, facilitate the cycling of NO to NO_2 (Zhang et al., 2002; Gligorovski et al., 2015). The

remaining CIs become collisionally stabilized Criegee intermediates (SCIs) that can undergo further bimolecular reactions with a number of atmospheric trace gases, such as H_2O, NO_2, and SO_2 (Chen et al., 2016a,b; Mauldin et al., 2012; Berndt et al., 2014; Kuwata et al., 2015; Lin et al., 2016; Ouyang et al., 2013; Stone et al., 2014; Chao et al., 2015; Lin et al., 2017; Taatjes et al., 2017; Long et al., 2018), and contribute to the nucleation and growth of secondary aerosol (e.g. nitrate, sulfate, SOAs) by partitioning between gas and particle phases (Foreman et al., 2016; Vereecken et al., 2017; Huang et al., 2015; Berndt et al., 2012; Zhang et al., 2015; Huang et al., 2014; Li et al., 2018; Ji et al., 2017; Xu et al., 2014). The bimolecular processes of SCIs at the air/water interface have been extensively studied both experimentally and theoretically (Zhu et al., 2016; Kumar et al., 2017, 2018; Zhong et al., 2017, 2018; Enami et al., 2017; Heine et al., 2017), and the reaction with atmosphere-abundant water vapour in the gas phase or at the air/water interface has been identified as one of the dominant degradation pathways of SCIs removal from the atmosphere (Chen et al., 2016a,b; Lin et al., 2016; Chao et al., 2015; Huang et al., 2015; Zhu et al., 2016; Zhong et al., 2017; Zhang et al., 2012; Taatjes et al., 2013; Anglada et al., 2016).

Experimentally, Su et al. (2013) investigated the transient infrared absorption spectrum of CH_2OO using a step-scan Fourier-transform spectrometer, and observed that the vibrational frequencies are more consistent with a zwitterion rather than a diradical structure. Taatjes et al. (2013) studied the kinetics of CH_3CHOO reactions with H_2O, SO_2, and NO_2, and found that *anti*-CH_3CHOO is substantially more reactive toward water and SO_2 than is *syn*-CH_3CHOO with an upper limit rate coefficient $(1.0 \pm 0.4) \times 10^{-14}$ cm^3 $molecule^{-1}$ s^{-1}. Also Smith et al. (2015) reached similar conclusions in their UV absorption of the $CH_2OO + H_2O$ reaction system that the rate coefficient is determined as $(7.4 \pm 0.6) \times 10^{-12}$ cm^3 $molecule^{-1}$ s^{-1} at 298 K, and it exhibits a large negative T-dependence at temperatures from 283 to 324 K. Moreover, oligomerization reactions of CIs with typical atmospheric species are identified as one of the dominate pathways leading to the formation of highly oxygenated and high-molecular-weight oligomers that have remarkably low vapor pressure contributing to SOAs formation and growth (Bonn et al., 2008; Heaton et al.,

Atmos. Chem. Phys. Discuss., https://doi.org/10.5194/acp-2018-935
Manuscript under review for journal Atmos. Chem. Phys.
Discussion started: 6 November 2018

2007; Wang et al., 2016; Inomata et al., 2014). For example, Sakamoto et al. (2013) performed laboratory-scale ethylene ozonolysis in a Teflon bag reactor, and revealed that the sequential addition of CH_2OO to hydroperoxides leads to oligomeric hydroperoxides and finally affords SOAs. Sadezky et al. (2008) proposed that SOAs formation is initiated by the reaction of SCI with a RO_2 radical, followed by the sequential addition of SCIs, and chain termination by reaction with HO_2 radical.

$$RO_2 + SCI \rightarrow RO_2\text{-}SCI \quad (1)$$

$$RO_2\text{-}SCI + (n\text{-}1)SCI \rightarrow RO_2\text{-}(SCI)_{n\text{-}1}\text{-}SCI \quad (2)$$

$$RO_2\text{-}(SCI)_{n\text{-}1}\text{-}SCI + HO_2 \rightarrow RO_2\text{-}(SCI)_n\text{-}H + O_2 \quad (3)$$

Zhao et al. (2015) studied the ozonolysis of *trans*-3-hexene in a flow reactor and static chambers in the absence and presence of an OH or SCI scavenger at 295 ± 1 K, arriving at the same conclusion as above. In particular, oligomers having SCIs as chain units were identified as one of the dominant components of atmospheric SOAs and were produced by the sequential addition of C_2H_5CHOO to RO_2 radical. More recently, Wang et al. (2016) investigated the heterogeneous ozonolysis of oleic acid (OL) using an aerosol flow tube, and found that reactions of particulate SCIs generate high-molecular-weight oligomers, with low volatility that are preferentially partitioned into the particle phase to promote SOAs formation. They confirmed that the SCI-based mechanism is dominant pathway in the formation of high-molecular-weight oligomers.

On the other hand, Ehn et al. (2014) reported a large source of low-volatility SOAs generated from the ozonolysis of α-pinene and other endocyclic monoterpenes under atmospheric conditions, and proposed that the mechanism of extremely low-volatility organic compounds (ELVOCs) formation is driven by RO_2 autoxidation. Also several groups reached similar conclusions that the highly oxygenated molecules (HOM) are produced via RO_2 autoxidation in the cyclohexene and terpenes ozonolysis systems (Rissanen et al., 2014; Kirkby et al., 2016; Berndt et al., 2018). Moreover, HOM are major contributors to aerosol particle formation and growth on a global scale (Tröstl et al., 2016; Stolzenburg et al., 2018). Compared with the RO_2

Atmos. Chem. Phys. Discuss., https://doi.org/10.5194/acp-2018-935
Manuscript under review for journal Atmos. Chem. Phys.
Discussion started: 6 November 2018

autoxidation pathways, oligomerization reactions involving CIs, preserve carbon oxidation state and increase carbon number, and therefore lead to a large reduction in volatility (Wang et al., 2016). Moreover, oligomerization reactions accompany with the shorter time period during the early stage of SOAs growth (Heaton et al., 2007). Therefore, we think that it is essential to investigate the Criegee chemistry-based mechanism of SOAs formation and growth.

Aplincourt et al. (2000) investigated the mechanism of CH_2OO reactions with CH_2O, H_2O, SO_2, and CO_2 at the CCSD(T) level of theory, and found that the reactions with H_2O, CH_2O, and SO_2 are preferable, whereas that with CO_2 is unlikely to occur. Because of the high concentration of H_2O ($[H_2O] \approx 7.0 \times 10^{17}$ molecules cm^{-3}) under atmospheric conditions (Zhang et al., 2014; Zhang et al., 2015), the reaction with water vapour is the dominant chemical sink (Aplincourt et al., 2000). Also Ryzhkov et al. (2003; 2004; 2006) reached similar conclusions that the most energetically favourable pathway of carbonyl oxide reaction with the water vapour is the formation of hydroxyalkyl hydroperoxide. Zhao et al. (2017) investigated the mechanisms and kinetics of four SCIs reactions with four RO_2 radicals, and found that the addition of terminal oxygen in RO_2 to central carbon in SCI is the most kinetically favourable channel. Unfortunately, there is very little study to do on the reactivity of SCIs toward hydroxyalkyl hydroperoxides (HHPs) generated from the reaction with water vapour. Moreover, the effect of substituents on the reactivity of carbonyl oxides is still poorly understood.

Recently, Vereecken et al. and Anglada et al. tried to mechanistically characterize the reaction of CH_2OO with CH_3OO radical using different quantum chemistry methods (Vereecken et al., 2012; Anglada et al., 2013), and revealed that the above reaction initially proceeds via the formation of a strong pre-reactive complex followed by a submerged electronic-energy barrier for the subsequent addition of the CH_3OO terminal oxygen atom to the CH_2OO central carbon atom. An analogous conclusion was obtained by investigating the reactions of *anti*-CH_3CHOO with HO_2 and H_2O_2 molecules, i.e., the sequential addition of SCIs is a favorable reaction mode for SOAs formation (Chen et al., 2017). Vereecken et al. (2017) also investigated the reactions

of CH_2OO with acids and enols using the CCSD(T)//M06-2X/aug-cc-pVTZ method, and found that the 1,4-insertion mechanism allows for barrierless reactions with high rate coefficients. The above milestone investigations provide fundamental insights and lay solid foundations for further studies of the Criegee chemistry-based mechanism of SOAs formation.

In this study, we mainly focus on the oligomerization reaction of carbonyl oxides with HHPs leading to the formation of high-molecular-weight oligomers under atmospheric conditions. This reaction represent the initial step of oligomer formation and growth during alkene ozonolysis, and therefore need to be extensively characterized to gain deeper insights into the fundamental chemical composition of these oligomers in the atmosphere. Moreover, structure-reactivity relationship plays an important role in determining the rates and outcomes of bimolecular processes. Herein, we employ high-level theoretical calculations in conjunction with kinetics analysis to study the mechanism and kinetics of the reactions of four carbonyl oxides with four HHPs, and describe the effects of carbonyl oxide conformation on reaction rate. The carbonyl oxides considered in this work (CH_2OO, *syn*-/*anti*-CH_3CHOO, and $(CH_3)_2COO$) are anticipated upon ozonolysis of ethylene, propylene, isobutene and 2,3-dimethyl-2-butene, while the investigated HHPs are assumed to arise from bimolecular reactions with water vapour in the troposphere.

2. Computational details

The geometries of all stationary points on PES are optimized and characterized by the M06-2X functional (Zhao et al., 2006) in combination with the 6-311+G(2df,2p) basis set (Zheng et al., 2009), since the M06-2X functional allows one to reliably compute the energies and stability of non-covalent interactions (Zhao et al., 2008a,b). Harmonic vibrational frequencies are performed at the same level of theory to verify that the nature of each structure is either a minimum (NIMAG = 0) or a transition state (NIMAG = 1) and to provide the zero point vibrational energy (ZPVE) corrections. A scale factor of 0.98 is applied to scale all the M06-2X/6-311+G(2df,2p) frequencies to account for the thermodynamic contribution

Atmos. Chem. Phys. Discuss., https://doi.org/10.5194/acp-2018-935
Manuscript under review for journal Atmos. Chem. Phys.
Discussion started: 6 November 2018

to the Gibbs free energy and enthalpy at 298 K and 1 atm (Zheng et al., 2009). The reactant-product connectivity on either side is established by intrinsic reaction coordinate (IRC) calculations (Fukui, 1981).

The barrier heights of some elementary reactions are calculated for single-point energies Y/X (Y = M06-2X, CCSD(T), X = 6-311+G(2df,2p), def2-TZVP) determined using M06-2X/6-311+G(2df,2p) optimized geometries. The obtained results (Table S1) indicate that the largest deviations of electronic-energy ($\Delta E_a^{\#}$) and free-energy ($\Delta G_a^{\#}$) barriers between CCSD(T)/6-311+G(2df,2p) and M06-2X/def2-TZVP methods are 1.6 and 1.5 kcal·mol^{-1}, respectively, while the respective mean absolute deviations (MAD) are 0.99 and 0.95 kcal·mol^{-1}. Thus, the M06-2X method afford energies similar to those determined by the accurate and well recognized CCSD(T) level calculation. Considering the computational costs, the M06-2X/def2-TZVP method is selected to perform the single-point energy calculation for the title reaction system. The rate coefficients are calculated using canonical transition state theory with quantum mechanical tunneling (Eckart) at temperatures relevant in the troposphere (273-400 K) in the high-pressure limit (Zhao et al., 2017; Chen et al., 2017).

$$k^{\mathrm{TST}}(T) = \sigma \frac{k_b T}{h} \left(\frac{\mathrm{R}T}{P^0}\right)^{\Delta n} \exp\left(\frac{-\Delta G^{\dagger}(T)}{k_b T}\right) \quad (4)$$

where $\Delta G^{\dagger}(T)$ is activation Gibbs free energy, σ is reaction symmetry number, k_b is Boltzmann's constant, T is the temperature in Kelvin, h is Planck's constant, and Δn= 0 and 1 for unimolecular and bimolecular reactions, respectively (Zhao et al., 2017). The quantum chemical calculations are executed using the Gaussian 09 program suite (Frisch et al., 2009). The rate coefficients are calculated by implementing the KiSThelP program (Canneaux et al., 2014).

3. Results and discussion

3.1 Bimolecular reaction of SCIs with water vapour

Equations (5) and (6) represent the two types of bimolecular reactions between carbonyl oxides and water vapour. Previous investigations have shown that some

Atmos. Chem. Phys. Discuss., https://doi.org/10.5194/acp-2018-935
Manuscript under review for journal Atmos. Chem. Phys.
Discussion started: 6 November 2018

carbonyl oxides are largely removed by their reactions with water dimer (Chen et al., 2016a,b; Chao et al., 2015; Taatjes et al., 2013; Anglada et al., 2016) to generate HHPs (Chen et al., 2016a,b; Anglada et al., 2011), which are important atmospheric oxidants initiating vegetation damage (Becker et al., 1990). Further mechanistic details of the above reaction can be found in our previous works (Chen et al., 2016a,b; 2018).

$$R_1R_2COO + H_2O \rightarrow R_1R_2C(OH)OOH \quad (5)$$

$$R_1R_2COO + (H_2O)_2 \rightarrow R_1R_2C(OH)OOH + H_2O \quad (6)$$

Figure 1 presents a simplified scheme for the reactions of several distinct carbonyl oxides (CH_2OO, *syn*-/*anti*-CH_3CHOO, $(CH_3)_2COO$) with water dimer to form HHPs. In all cases, each reaction begins with the formation of a strong pre-reactive complex and then surmounts a small barrier that is still lower in energy than the reactants before product generation. Table 1 contains the relative energies of stationary points and the activation energies of elementary reactions. In Figure 1 and Table 1, labels A, B, C, and D correspond to the relative energies of the pre-reactive complex (RC), transition state (TS), post-reactive complex (PC) and the product (P). R1 and R2 denote *syn*- and *anti*-positions of the substituent, respectively. These four transition states are located by rotation of two dihedral angles (DO2H4O4H3, DO4H2O3H1). Based on the energies given in Table 1, products **Pa** and **Pb** are near-isoenergetic conformers differing only in the orientation of the H1 atom along the C1-O3 bond. As has been mentioned above, HHPs are key reactive intermediates that possess with -OH and -OOH functional groups, and can therefore sequentially react with carbonyl oxide to generate oligomers. Considering the fact that Pa and Pb are structurally and energetically similar, the former is judiciously selected for studying oligomerization reactions, whereas the latter is merely listed in the Figures S1-S3.

3.2 PES for the reaction of CH_2OO with $HO\text{-}CH_2OO\text{-}H$

CH_2OO, the simplest Criegee intermediate, originates from the ozonolysis of all exocyclic alkenes, e.g., isoprene, monoterpenes, and sesquiterpenes (Nguyen et al.,

246 2016), which makes its chemistry particular important for forest and urban
247 environments. The largest sink of CH_2OO corresponds to its bimolecular reaction
248 with water dimer in the troposphere, which generates HO-CH_2OO-H as the dominant
249 product (Lewis et al., 2015; Kumar et al., 2014). Figure 2 shows the schematic PES
250 for the reaction of CH_2OO with HO-CH_2OO-H, with the optimized geometries of all
251 stationary points on this PES given in Figure S4.

252 Figure 2 shows that the differences between the relative free energies and the
253 electronic energies for all stationary points are significant (~ 10-24 kcal mol^{-1}),
254 implying that the addition reactions of the parent carbonyl oxide with Pa_1 are
255 characterized by obvious contributions of entropy effect. Similar behaviors are also
256 observed for oligomerization reactions of other carbonyl oxides with HHPs (see
257 Figures 3-5). Thus, unless otherwise stated, the discussion in the following sections
258 refers to free-energy barriers ($\Delta G_a^{\#}$).

259 The formation of oligomers P2a, P2b, P2c and P2d (containing CH_2OO as the
260 repeating unit) is strongly exothermic (>104 kcal mol^{-1}), and the apparent activation
261 energies E_{app} observed for all elementary reactions are negative values, signifying that
262 these reactions are both thermochemically and dynamically feasible under
263 atmospheric condition. Product Pa_1 (HO-CH_2OO-H) formed in the reaction of CH_2OO
264 with water dimer has two functional groups (-OH and -OOH), both of which can be
265 involved in addition reactions. The addition reactions of $2CH_2OO$ + Pa_1 begin with
266 the formation of loosely bound pre-reactive complexes IM1a and IM1b, of -3.5 and
267 -3.1 kcal mol^{-1} stability. They are formed by a hydrogen bond between the terminal
268 CH_2OO oxygen atom and the hydrogen atom of the -OOH group in Pa_1, and a van der
269 Waals (vdW) bond between the central carbon atom of CH_2OO and the oxygen atom
270 of the -OH group in Pa_1. The above complexes are immediately converted into
271 products P1a and P1b via transition states TS1a and TS1b with barriers of 8.8 and
272 12.2 kcal mol^{-1}, respectively, while the corresponding reaction exothermicities are
273 estimated as 43.4 and 40.5 kcal mol^{-1}, respectively. The above result shows that the
274 most favorable channel is the addition of the -OOH group of Pa_1 to the parent
275 carbonyl oxide. The detailed mechanism mainly involves that the HO-CH_2OO moiety

Atmos. Chem. Phys. Discuss., https://doi.org/10.5194/acp-2018-935
Manuscript under review for journal Atmos. Chem. Phys.
Discussion started: 6 November 2018

released from the breaking O-H bond in Pa_1 binds to the central carbon atom of CH_2OO, and simultaneously the remnant hydrogen atom transfers to the terminal oxygen leading to product P1a.

The addition pathway opens the door for other subsequent reactions leading to SOAs via Criegee chemistry, which may result in aerosol formation and thus impact climate. As pointed out in previous studies (Chen et al., 2016a,b; Kumar et al., 2014), the thermal unimolecular decay of Pa_1 can occur via two competitive pathways, namely (i) HO-CH_2OO-H → CH_2O + H_2O_2 and (ii) HO-CH_2OO-H → HCOOH + H_2O. However, since the corresponding barriers are much higher than that of the bimolecular reaction with CH_2OO (~35 kcal·mol^{-1}), the thermal unimolecular decay of HHPs is not taken into consideration in this work.

The secondary addition reaction CH_2OO + P1a is equivalent to that of CH_2OO + Pa_1 reaction, and hence features an analogous pathway, i.e., the formation of pre-reactive complexes IM2a and IM2b in entrance channels, is followed by the addition of -OH and -OOH groups of P1a to the CH_2OO central carbon atom to produce P2a and P2b. The barrier heights predict TS2a and TS2b to lie -36.3 and -35.9 kcal·mol^{-1}, respectively, below the energies of the separate reactants, and 7.5 and 7.4 kcal·mol^{-1} above the energies of the corresponding pre-reactive complexes IM2a and IM2b. The above result shows that these two addition reactions (R2a and R2b) equally contribute to the title reaction system. Compared to the first CH_2OO addition reaction, the second one features a lower barrier. Finally, the addition reaction CH_2OO + P1b proceeds via mechanism fairly similar to those described above for the CH_2OO + P1a system and do not discussing in detail to avoid redundancy.

3.3 PES for the reaction of CH_3CHOO with HO-CH_3CHOO-H

The methyl-substituted parent Criegee intermediate can exist in two conformations, *syn*- and *anti*-CH_3CHOO, depending on whether the methyl group is located on the same or opposite side of the terminal oxygen (Yin et al., 2017). Numerous theoretical studies have proven that the presence of an intramolecular

Atmos. Chem. Phys. Discuss., https://doi.org/10.5194/acp-2018-935
Manuscript under review for journal Atmos. Chem. Phys.
Discussion started: 6 November 2018

Atmospheric Chemistry and Physics Discussions

hydrogen bond in the *syn*-conformer makes it more stable than the *anti*-conformer (Anglada et al., 2011; 2016). The interconversion of these two conformers via rotation around the C-O bond has a very high barrier (~ 42 kcal mol^{-1}), which implies that one can treat *syn*- and *anti*-CH_3CHOO as independent species existing in the atmosphere (Yin et al., 2017). It is well known that the predominant pathway of unimolecular reaction of *syn*-CH_3CHOO is isomerization to vinyl hydroperoxide (VHP) via the hydrogen atom transfer, whereas the preferable route of unimolecular reaction of *anti*-CH_3CHOO is ring-closure to dioxirane via an oxygen atom transfer (Donahue et al., 2011; Taatjes et al., 2013; Long et al., 2016). Both of the prompt and thermal unimolecular decay of the energized VHP may dissociate to OH radicals, and their yields are strongly pressure and temperature dependents (Kroll et al., 2011a,b). The dioxirane can finally isomerize to acetic acid via the "hot acid" channel (Kroll et al., 2011a,b).

Long et al. (2016) proposed that the enthalpic barrier of *syn*-CH_3CHOO isomerization to VHP is more than ~3 kcal higher than that of the addition reaction *syn*-CH_3CHOO + H_2O, indicating that the latter reaction is the dominant pathway. Also Taatjes et al. (2013) reached same conclusions that CH_3CHOO reaction with water is the dominate tropospheric removal pathway. Moreover, the high rate coefficients of the reactions of CH_3CHOO with water vapour (Taatjes et al., 2013; Anglada et al., 2011; 2016) (k(*syn*-CH_3CHOO + H_2O) = 4.0×10^{-15} cm^3 $molecule^{-1}$ s^{-1}, k(*anti*-CH_3CHOO + H_2O) = $1.0 \pm 0.4 \times 10^{-14}$ cm^3 $molecule^{-1}$ s^{-1}) suggest that water can effectively scavenge CH_3CHOO to generate low volatile HO-C(CH_3)HOO-H and thus promote SOAs formation. The energy diagram of addition reactions between CH_3CHOO and HO-C(CH_3)HOO-H is given in Figure 3. The optimized geometries of all stationary points are shown in Figures S5 and S6.

Figure 3(a) demonstrates that the sequential additions of *anti*-CH_3CHOO to Pa_2 are strongly exothermic and spontaneous, indicating that the occurrence of these consecutive reactions in the atmosphere is thermochemically feasible. The addition reactions of 2*anti*-CH_3CHOO + Pa_2 start with the barrierless formation of pre-reactive complexes IM3a and IM3b held together by weak hydrogen bonds and vdW forces.

Atmos. Chem. Phys. Discuss., https://doi.org/10.5194/acp-2018-935
Manuscript under review for journal Atmos. Chem. Phys.
Discussion started: 6 November 2018

Atmospheric Chemistry and Physics Discussions

335 Subsequently, the -OH and -OOH fragments in Pa_2 immediately add to the central
336 carbon atom of *anti*-CH_3CHOO to produce P3a and P3b. The barriers of these two
337 addition reactions are 6.2 and 8.8 kcal mol^{-1} with the concomitant release 39.5 and
338 34.1 kcal mol^{-1} of energies. This result confirms that the most favorable channel, both
339 thermochemically and dynamically, corresponds to the -OOH group addition pathway.
340 Notably, the above reaction barriers are lower than that of the $2CH_2OO + Pa_1$ system
341 by ~ 3.0 kcal mol^{-1}, indicating that *anti*-CH_3CHOO is significantly more reactive than
342 the parent carbonyl oxide. This finding is further corroborated by the results of
343 Anglada et al. (2016) and Chen et al., (2017) who found that CH_2OO is significantly
344 less reactive than *anti*-CH_3CHOO towards H_2O, HCOOH, and CH_3COOH.

345 The addition reaction *anti*-$CH_3CHOO + Pa_2$ results in the formation of P3a,
346 which can subsequently react with *anti*-CH_3CHOO via channels R4a and R4b. Both
347 of these pathways start with the formation of pre-reactive complexes IM4a and IM4b
348 in entrance channels, that is followed by the addition of -OH and -OOH groups of P3a
349 to the central carbon atom of *anti*-CH_3CHOO to produce P4a and P4b. According to
350 the predicted barrier heights, TS4a and TS4b lie 7.3 and 16.7 kcal mol^{-1} above
351 complexes IM4a and IM4b, respectively, which re-confirms that the most favorable
352 reaction channel is the -OOH group addition pathway.

353 At this point, it is worth noting that the addition reactions in the 2*syn*-CH_3CHOO
354 + $Pa_{2'}$ system proceed through a similar mechanism and are thus only briefly
355 discussed in the following section. As revealed by Figure 3(b), both R5a and R5b
356 pathways start with the formations of vdW complexes IM5a and IM5b, that are
357 spontaneously converted into products P5a and P5b. The barriers of these two
358 addition reactions are estimated as 12.5 and 12.0 kcal mol^{-1}, respectively, and are
359 therefore significantly higher than those calculated for comparable 2*anti*-CH_3CHOO
360 + Pa_2 system. This discrepancy is ascribed to the fact that the steric repulsion between
361 the methyl group and the terminal oxygen in *syn*-CH_3CHOO results in decreased
362 hydrogen transfer ability and hinders the formation of pre-reactive complexes.

363 The above result is further supported by recent reports, which claim the
364 *syn*-conformer to be substantially less reactive than the *anti*-conformer toward key

Atmos. Chem. Phys. Discuss., https://doi.org/10.5194/acp-2018-935
Manuscript under review for journal Atmos. Chem. Phys.
Discussion started: 6 November 2018

atmospheric species, such as H_2O, SO_2 and NO_2 (Taatjes et al., 2013; Anglada et al., 2011; Sheps et al., 2014). The lowest-energy channel among the P5a/P5b + *syn*-CH_3CHOO reaction pathways, TS6a, involves the addition of the -OOH group with a barrier of only 11.0 kcal mol^{-1} and a large exothermicity of ~ 40 kcal mol^{-1}.

3.4 PES for the reaction of $(CH_3)_2COO$ with HO-$(CH_3)_2$COO-H

The dimethyl-substituted Criegee intermediate $(CH_3)_2COO$ is generated in the ozonolysis of 2,3-dimethyl-2-butene (Lester et al., 2018; Drozd et al., 2017). The unimolecular reaction of $(CH_3)_2COO$ and its bimolecular reaction with water vapour strongly depend on temperature (Long et al., 2018). For example, the unimolecular reaction is the dominant decay pathway above 240 K, whereas it reaction with SO_2 can compete well with the corresponding unimolecular reaction below 240 K (Long et al., 2018). Although a fraction of $(CH_3)_2COO$ may proceed unimolecular decomposition or react with SO_2 under some specific conditions, the removal of this species from the atmosphere mainly occurs via its reaction with water vapour due to its higher atmospheric concentration (Kuwata et al., 2015; Long et al., 2018; Huang et al., 2015), which afford HO-C$(CH_3)_2$OO-H as the major product. The PES of addition reactions $(CH_3)_2COO$ + HO-C$(CH_3)_2$OO-H is given in Figure 4, and the optimized geometries of all stationary points are shown in Figure S7.

As shown in Figure 4, the vdW complexes IM7a and IM7b are 5.0 and 5.1 kcal mol^{-1} lower in energy than the reactants, while the corresponding transition states TS7a and TS7b leading to products P7a and P7b are 10.3 and 14.2 kcal mol^{-1} higher in energy than the respective complexes. The formation of P7a and P7b is strongly exothermic, with the reaction energies of -31.0 and -25.8 kcal mol^{-1}. Again, this result shows that the addition of the -OOH group in Pa_3 to the central carbon atom of $(CH_3)_2COO$ is both thermochemically and dynamically favorable. Compared with the barriers of 2*anti*-CH_3CHOO + Pa_2 system given in Figure 3(a), one can notice that the dimethyl-substituted parent carbonyl oxide leads to the barrier increasing by ~ 5 kcal mol^{-1}. The secondary addition reaction $(CH_3)_2COO$ + P7a is found to be similar to that described for the $(CH_3)_2COO$ + Pa_3 system. The pre-reactive complexes IM8a

Atmos. Chem. Phys. Discuss., https://doi.org/10.5194/acp-2018-935
Manuscript under review for journal Atmos. Chem. Phys.
Discussion started: 6 November 2018

and IM8b are formed in entrance channels with over 5.0 kcal mol^{-1} stabilization energies, and followed by the addition of -OH and -OOH groups in P7a to the central carbon atom of $(CH_3)_2COO$ to generate P8a and P8b. According to the predicted barrier heights, TS8a and TS8b lie 12.0 and 13.0 kcal mol^{-1} above complexes IM8a and IM8b, respectively, which shows that the second addition reactions R8a and R8b are nearly equally accessible.

3.5 PES of distinct SCI reactions with HO-CH_2OO-H

To gain deeper insights into the substituent-influenced modification atmospheric oligomer composition, one should elucidate the origin of the substituent influence on the reactivity and kinetics of carbonyl oxides. Therefore, an understanding of structure-reactivity relationships is important for determining bimolecular processes and reaction products. Since the addition of the -OOH group to the central carbon atom of SCIs is shown to be both thermochemically and dynamically preferable, this type of addition reaction is selected to study the effect of substituents on the reactivity of carbonyl oxides. The PES of addition reactions SCIs + HO-CH_2OO-H is given in Figure 5, whereas those for bimolecular reactions with other HHPs are displayed in Figures S8-S10.

As shown in Figure 5, each reaction begins with the formation of a strong pre-reactive complex and then surmounts a medium barrier that is higher in energy relative to the reactants before forming the corresponding products. The bimolecular reaction of CH_2OO with HO-CH_2OO-H to form P1a(HO-$(CH_2OO)_2$-H) is characterized by a barrier of 8.8 kcal mol^{-1} and an exothermicity of 43.4 kcal mol^{-1}. Hence, the small barrier and large stability of the hydroperoxide species imply that its formation is both thermochemically and kinetically favoured. Notably, the introduction of a methyl group at the *anti*-position reduces the barrier by ~ 1.0 kcal mol^{-1} relative to that of the CH_2OO + HO-CH_2OO-H system, whereas the corresponding *syn*- and dimethyl substitutions increase the above barrier by 4.2 and 3.3 kcal mol^{-1}, respectively. These results indicate that the *anti*-conformer is substantially more reactive toward HO-CH_2OO-H than *syn*-, dimethyl- and parent

Atmos. Chem. Phys. Discuss., https://doi.org/10.5194/acp-2018-935
Manuscript under review for journal Atmos. Chem. Phys.
Discussion started: 6 November 2018

conformers in the atmosphere. A similar conclusion has been obtained by studying the reactions of *syn*-/*anti*-CH_3CHOO with water and SO_2, i.e., the rate coefficient of the *anti*-CH_3CHOO reaction was calculated to be one to two orders of magnitude higher than that of the *syn*-CH_3CHOO system (Lin et al., 2016; Huang et al., 2015; Taatjes et al., 2013; Anglada et al., 2016). Therefore, it is concluded that the position and number of methyl groups significantly affect barrier heights and reaction rates. On the other hand, the exothermicities of other reaction pathways are lower than that of the parent system, which implies that methyl substitution is thermochemically unfavorable. A similar trend is observed for the bimolecular reactions of SCIs with other HHPs (Figures S8-S10). In order to avoid redundancy, we do not repeat them here in detail.

3.6 Kinetics and implications in atmospheric chemistry

To better understand the effect of substituents on reaction kinetics, the rate coefficients of distinct SCI reactions with HO-CH_2OO-H are computed using a combination of canonical transition state theory and Eckart tunneling correction at temperatures between 273 and 400 K, with the obtained results listed in Table 2.

Table 2 shows that the predicted rate coefficients for the reaction of CH_2OO with HO-CH_2OO-H(R1a) decrease with increasing temperature, with a similar trend observed for *syn*-CH_3CHOO(R9), *anti*-CH_3CHOO(R10), and $(CH_3)_2COO$ + HO-CH_2OO-H(R11) systems. The above behavior is ascribed to the fact that the apparent activation barriers E_{app} of these four addition reactions are significantly negative, as previously observed for the reaction of CH_3O_2 with BrO (Shallcross et al., 2015). These findings imply that a significant fraction of atmospheric carbonyl oxides may survive under high temperature conditions and react with peroxy radical or organic acid to generate SOAs.

The obtained data shows that the rate coefficient depends on the relative position and number of methyl groups in the parent carbonyl oxide, e.g., the rate coefficient increases by two orders of magnitude when methyl substitution occurs at the *anti*-position, whereas a reduction by four orders of magnitude is observed for methyl

452 substitution at the *syn*-position. Thus, the relative position of the methyl group plays
453 an important role in determining SCI reactivity, in particular, *anti*-substitution
454 promotes the reaction with HHPs and accelerates the formation of oligomers in the
455 atmosphere. Anglada et al. arrived at the same conclusion by studying the reactions of
456 SCIs with water vapour, showing that the *anti*-conformer is significantly more
457 reactive than the parent carbonyl oxide and the *syn*-conformer (Anglada et al., 2011;
458 2016). On the other hand, the introduction of two methyl groups does not result in a
459 marked rate coefficient change compared to the parent system, since the addition
460 reaction R11 is mediated by the pre-reactive hydrogen-bonded complex.

461 As discussed above, the reaction of *anti*-CH_3CHOO with HO-CH_2OO-H is
462 preferred over the other three pathways. Therefore, it would be interesting to
463 investigate whether the reaction between *anti*-CH_3CHOO and HO-CH_2OO-H can
464 compete with the reaction between *anti*-CH_3CHOO and formic acid, which represents
465 a substantially dominant atmospheric degradation pathway (Welz et al., 2014).
466 Assuming that the concentration of HO-CH_2OO-H is approximately equal to that of
467 SCIs (~5.0×10^4 molecules cm^{-3}; within an order of magnitude uncertainty) in the
468 boreal forest and rural environments of Finland and Germany (Novelli et al., 2016,
469 2017), the lifetime of *anti*-CH_3CHOO can be calculated as 5.9×10^3 s. The rate
470 coefficient of the bimolecular reaction of *anti*-CH_3CHOO with HCOOH
471 approximately equals $(5 \pm 3) \times 10^{-10}$ cm^3 $molecule^{-1}$ s^{-1} at 298 K (Welz et al., 2014),
472 corresponding to an estimated *anti*-CH_3CHOO lifetime of ~ 0.03 s at an average
473 daytime concentration of [HCOOH] = 2.0×10^{11} molecules cm^{-3} (Zhang et al., 2014).
474 Therefore, the *anti*-CH_3CHOO + HO-CH_2OO-H reaction may not compete with the
475 *anti*-CH_3CHOO + HCOOH reaction during daytime. However, the concentration of
476 formic acid dramatically decreases in the nighttime, allowing the *anti*-CH_3CHOO +
477 HO-CH_2OO-H reaction to compete with the *anti*-CH_3CHOO + HCOOH reaction at
478 temperatures below 273 K when the concentration of HCOOH equals 9.0×10^7
479 molecules cm^{-3}.

480 ## 4. Conclusion

The reactivity and kinetics of oligomerization reactions of Criegee intermediates with HHPs are studied using quantum-chemical methodologies in conjunction with statistical theory calculations. The main conclusions are summarized as follows:

(a) The oligomerization reactions of SCIs with HHPs are strongly exothermic and spontaneous, signifying that the consecutive reactions are feasible thermochemically in the atmosphere.

(b) The addition of -OOH group in HHPs to the central carbon atom of SCIs is both thermochemically and dynamically preferable as compared with the -OH group addition pathway.

(c) The reaction barrier and kinetics strongly depend on both, the number of the substituents in the Criegee intermediate and on its position (*syn*- or *anti*-).

(d) The rate coefficients show a significant increase when adding a methyl group on the *anti*-position, whereas it displays a dramatical decrease on the *syn*-position. On the other hand, the addition of dimethyl group does not cause much variation in the rate coefficients.

Acknowledgments

This work was supported by the National Key Research and Development Program of China (2016YFA0203000) and the National Natural Science Foundation of China (Nos. 41573138, 21473108 and 41805107). It was also partially supported by the Key Project of International Cooperation of the Chinese Academy of Sciences (GJHZ1543), Research Grants Council of Hong Kong (PolyU 152083/14E), Open Foundation of State Key Laboratory of Loess and Quaternary Geology (SKLLQG1627), and Shaanxi Province Postdoctoral Science Foundation (No. 2017BSHEDZZ62). Yu Huang is also supported by the "Hundred Talent Program" of the Chinese Academy of Sciences.

Supporting Information

The barriers for the addition reactions of carbonyl oxides with HHPs; PESs for addition reactions of CH_2OO + HO-CH_2OO-H(Pb_1), *syn*-/*anti*-CH_3CHOO + HO-C(CH_3)HOO-H, $(CH_3)_2COO$ + HO-C(CH_3)$_2$OO-H (Pb_3), SCIs +

510 HO-CH(CH_3)OO-H(Pa_2), SCIs + HO-CH(CH_3)OO-H($Pa_{2'}$) and SCIs +
511 HO-C(CH_3)$_2$OO-H; optimized geometries of all the stationary points.
512
513
514 Competing interests. The authors declare that they have no conflict of interest.
515 Author contributions. LC designed the study. LC and YH wrote the paper. LC
516 performed theoretical calculation. YX, ZS, JC, and WW analyzed the data. All authors
517 reviewed and commented on the paper.
518

References

Anglada, J. M., and Solé, A.: Impact of water dimer on the atmospheric reactivity of carbonyl oxides, Phys. Chem. Chem. Phys., 18, 17698-17712, 10.1039/c6cp02531e, 2016.

Anglada, J. M., González, J., and Torrent-Sucarrat, M.: Effects of the substituents on the reactivity of carbonyl oxides. A theoretical study on the reaction of substituted carbonyl oxides with water, Phys. Chem. Chem. Phys., 13, 13034-13045, 10.1039/c1cp20872a, 2011.

Anglada, J. M., Olivella, S., and Solé, A.: The reaction of formaldehyde carbonyl oxide with the methyl peroxy radical and its relevance in the chemistry of the atmosphere, Phys. Chem. Chem. Phys., 15, 18921-18933, 10.1039/c3cp53100g, 2013.

Aplincourt, P., and Ruiz-López, M. F.: Theoretical investigation of reaction mechanisms for carboxylic acid formation in the atmosphere, J. Am. Chem. Soc., 122, 8990-8997, 10.1021/ja000731z, 2000.

Becker, K. H., Brockmann, K. J., and Bechara, J.: Production of hydrogen peroxide in forest air by reaction of ozone with terpenes, Nature, 346, 256-258, 10.1038/346256a0, 1990.

Berndt, T., Jokinen, T., Mauldin, R. L., Petäjä, T., Herrmann, H., Junninen, H., Paasonen, P., Worsnop, D. R., and Sipilä, M.: Gas-phase ozonolysis of selected olefins: the yield of stabilized Criegee intermediate and the reactivity toward SO_2, J. Phys. Chem. Lett., 3, 2892-2896, 10.1021/jz301158u, 2012.

Berndt, T., Scholz, W., Mentler, B., Fischer, L., Herrmann, H., Kulmala, M., and Hansel, A.: Accretion productformation from self- and cross-reactions of RO_2 radicals in the atmosphere, Angew. Chem. Int. Ed., 57, 3820-3824, 10.1002/anie.201710989, 2018.

Berndt, T., Voigtländer, J., Stratmann, F., Junninen, H., Mauldin, I. R. L., Sipilä, M., Kulmala, M., and Herrmann, H.: Competing atmospheric reactions of CH_2OO with SO_2 and water vapour, Phys. Chem. Chem. Phys., 16, 19130-19136, 10.1039/c4cp02345e, 2014.

Bonn, B., Kulmala, M., Riipinen, I., Sihto, S. L., and Ruuskanen, T. M.: How biogenic terpenes govern the correlation between sulfuric acid concentrations and new particle formation, J. Geophys. Res. Atmos., 113, D12209, 10.1029/2007JD009327, 2008.

Canneaux, S., Bohr, F., and Henon, E.: KiSThelP: A program to predict thermodynamic properties and rate constants from quantum chemistry results, J. Comput. Chem., 35, 82-93, 10.1002/jcc.23470, 2014.

Chao, W., Hsieh, J. T., Chang, C. H., and Lin, J. J. M.: Direct kinetic measurement of the reaction of the simplest Criegee intermediate with water vapor, Science, 347, 751-4, 10.1126/science.1261549, 2015.

Chen, L., Huang, Y., Xue, Y., Cao, J. J., and Wang, W.: Competition between HO_2 and H_2O_2 reactions with CH_2OO/anti-CH_3CHOO in the oligomer formation: a theoretical perspective, J. Phys. Chem. A, 121, 6981-6991, 10.1021/acs.jpca.7b05951, 2017.

Chen, L., Huang, Y., Xue, Y., Cao, J. J., and Wang, W.: Effect of oligomerization reactions of Criegee intermediate with organic acid/peroxy radical on secondary organic aerosol formation from isoprene ozonolysis, Atmos. Environ., 187, 218-229, 10.1016/j.atmosenv.2018.06.001, 2018.

Chen, L., Wang, W. L., Wang, W. N., Liu, Y. L., Liu, F. Y., Liu, N., and Wang, B. Z.: Water-catalyzed decomposition of the simplest Criegee intermediate CH_2OO, Theor. Chem. Acc., 135, 131-143, 10.1007/s00214-016-1894-9, 2016.

562 Chen, L., Wang. W. L., Zhou, L. T., Wang, W. N., Liu, F. Y., Li, C. Y., and Lü, J.: Role of water
563 clusters in the reaction of the simplest Criegee intermediate CH_2OO with water vapour, Theor.
564 Chem. Acc., 135, 252-263, 10.1007/s00214-016-1998-2, 2016.
565 Criegee, R.: Mechanism of ozonolysis, Angew. Chem. Int. Ed. Engl., 14, 745-752,
566 10.1002/anie.197507451, 1975.
567 Donahue, N. M., Drozd, G. T., Epstein, S. A., Presto, A. A., and Kroll, J. H.: Adventures in
568 ozoneland: down the rabbit-hole, Phys. Chem. Chem. Phys., 13, 10848-10857,
569 10.1039/c0cp02564j, 2011.
570 Donahue, N. M., Kroll, J. H., Pandis, S. N., and Robinson, A. L.: A two-dimensional volatility
571 basis set – Part 2: Diagnostics of organic-aerosol evolution, Atmos. Chem. Phys., 12,
572 615-634, 10.5194/acp-12-615-2012, 2012.
573 Donahue, N. M., Trump, E. R., Pierce, J. R., and Riipinen, I.: Theoretical constraints on pure
574 vapor-pressure driven condensation of organics to ultrafine particles, Geophys. Res. Lett., 38,
575 L16801, 10.1029/2011GL048115, 2011.
576 Drozd, G. T., Kurtén, T., Donahue, N. M., and Lester, M. I.: Unimolecular decay of the
577 dimethyl-substituted Criegee intermediate in alkene ozonolysis: decay time scales and the
578 importance of tunneling, J. Phys. Chem. A, 121, 6036-6045, 10.1021/acs.jpca.7b05495, 2017.
579 Ehn, M., Thornton, J. A., Kleist, E., Sipilä, M., Junninen, H., Pullinen, I., Springer, M., Rubach, F.,
580 Tillmann, R., Lee, B., Lopez-Hilfiker, F., Andres, S., Acir, I. H., Rissanen, M., Jokinen,T.,
581 Schobesberger, S., Kangasluoma, J., Kontkanen, J., Nieminen, T., Kurtén, T., Nielsen, L. B.,
582 Jørgensen, S., Kjaergaard, H. G., Canagaratna, M., Maso, M. D., Berndt, T., Petäjä, T.,
583 Wahner, A., Kerminen, V. M., Kulmala, M., Worsnop, D. R., Wildt, J., and Mentel T. F.: A
584 large source of low-volatility secondary organic aerosol, Nature, 506, 476-9,
585 10.1038/nature13032, 2014.
586 Enami, S., and Colussi, A. J.: Reactions of Criegee intermediates with alcohols at air-aqueous
587 interfaces, J. Phys. Chem. A, 121, 5175-5182, 10.1021/acs.jpca.7b04272, 2017.
588 Foreman, E. S., Kapnas, K. M., and Murray, C.: Reactions between Criegee intermediates and the
589 inorganic acids HCl and HNO_3: kinetics and atmospheric implications, Angew. Chem. Int.
590 Ed., 55, 10419-10422, 10.1002/anie.201604662, 2016.
591 Frisch, M. J., Trucks, G. W., Schlegel, H. B., Scuseria, G. E., Robb, M. A., Cheeseman, J. R.,
592 Montgomery, J. A. Jr., Vreven, T., Kudin, K. N., Burant, J. C., Millam, J. M., Iyengar, S. S.,
593 Tomasi, J., Barone, V., Mennucci. B., Cossi, M., Scalmani, G., Rega, N., Petersson, G. A.,
594 Nakatsuji, H., Hada, M., Ehara, M., Toyota, K., Fukuda, R., Hasegawa, J., Ishida, M.,
595 Nakajima, T., Honda, Y., Kitao, O., Nakai, H., Klene, M., Li, X., Knox, J. E., Hratchian, H. P.,
596 Cross, J. B., Adamo, C., Jaramillo, J., Gomperts, R., Stratmann, R. E., Yazyev, O., Austin, A.
597 J., Cammi, R., Pomelli, C., Ochterski, J. W., Ayala, P. Y., Morokuma, K., Voth, G. A.,
598 Salvador, P., Dannenberg, J. J., Zakrzewski, V. G., Dapprich, S., Daniels, A. D., Strain, M. C.,
599 Farkas, O., Malick, D. K., Rabuck, A. D., Raghavachari, K., Foresman, J. B., Ortiz, J. V., Cui,
600 Q., Baboul, A. G., Clifford, S., Cioslowski, J., Stefanov, B. B., Liu, G., Liashenko, A.,
601 Piskorz, P., Komaromi, I., Martin, R. L., Fox, D. J., Keith, T., Al-Laham, M. A., Peng, C. Y.,
602 Nanayakkara, A., Challacombe, M., Gill, P. M. W., Johnson, B., Chen, W., Wong, M. W.,
603 Gonzalez, C., and Pople, J. A.: Gaussian 09, Revision D.01; Gaussian, Inc.: Wallingford, CT,
604 2009.
605 Fukui, K.: The path of chemical reactions - the IRC approach, Acc. Chem. Res., 14, 363-368,

606 10.1021/ar00072a001, 1981.
607 Gligorovski, S., Strekowski, R., Barbati, S., and Vione, D.: Environmental implications of
608 hydroxyl radicals (•OH), Chem. Rev., 115, 13051-13092, 10.1021/cr500310b, 2015.
609 Green, A. M., Barber, V. P., Fang, Y., Klippenstein, S. J., and Lester, M. I.: Selective deuteration
610 illuminates the importance of tunneling in the unimolecular decay of Criegee intermediates to
611 hydroxyl radical products, Proc. Natl. Acad. Sci. U.S.A., 114, 12372-12377,
612 10.1073/pnas.1715014114, 2017.
613 Hallquist, M., Wenger, J. C., Baltensperger, U., Rudich, Y., Simpson, D., Claeys, M., Dommen, J.,
614 Donahue, N. M., George, C., Goldstein, A. H., Hamilton, J. F., Herrmann, H., Hoffmann, T.,
615 Iinuma, Y., Jang, M., Jenkin, M. E., Jimenez, J. L., Kiendler-Scharr, A., Maenhaut, W.,
616 McFiggans, G., Mentel, Th. F., Monod, A., Prévôt, A. S. H., Seinfeld, J. H., Surratt, J. D.,
617 Szmigielski, R., and Wildt, J.: The formation, properties and impact of secondary organic
618 aerosol: current and emerging issues, Atmos. Chem. Phys., 9, 5155-5236,
619 10.5194/acp-9-5155-2009, 2009.
620 Heaton, K. J., Dreyfus, M. A., Wang, S., and Johnston, M. V.: Oligomers in the early stage of
621 biogenic secondary organic aerosol formation and growth, Environ. Sci. Technol., 41,
622 6129-6136, 10.1021/es070314n, 2007.
623 Heine, N., Houle, F. A., and Wilson, K. R.: Connecting the elementary reaction pathways of
624 Criegee intermediates to the chemical erosion of squalene interfaces during ozonolysis,
625 Environ. Sci. Technol., 51, 13740-13748, 10.1021/acs.est.7b04197, 2017.
626 Huang, H. L., Chao, W., and Lin, J. J. M.: Kinetics of a Criegee intermediate that would survive
627 high humidity and may oxidize atmospheric SO_2, Proc. Natl. Acad. Sci. U.S.A., 112,
628 10857-10862, 10.1073/pnas.1513149112, 2015.
629 Huang, R. J., Zhang, Y., Bozzetti, C., Ho, K. F., Cao, J. J., Han, Y., Daellenbach, K. R., Slowik, J.
630 G., Platt, S. M., Canonaco, F., Zotter, P., Wolf, R., Pieber, S. M., Bruns, E. A., Crippa, M.,
631 Ciarelli, G., Piazzalunga, A., Schwikowski, M., Abbaszade, G., Schnelle-Kreis, J.,
632 Zimmermann, R., An, Z., Szidat, S., Baltensperger, U., Haddad, I. E., Prévôt, A. S. H.: High
633 secondary aerosol contribution to particulate pollution during haze events in China, Nature,
634 514, 218-222, 10.1038/nature13774, 2014.
635 Inomata, S., Sato, K., Hirokawa, J., Sakamoto, Y., Tanimoto, H., Okumura, M., Tohno, S., and
636 Imamura, T.: Analysis of secondary organic aerosols from ozonolysis of isoprene by proton
637 transfer reaction mass spectrometry, Atmos. Environ., 97, 397-405,
638 10.1016/j.atmosenv.2014.03.045, 2014.
639 Ji, Y., Zhao, J., Terazono, H., Misawa, K., Levitt, N. P., Li, Y., Lin, Y., Peng, J., Wang, Y., Duan, L.,
640 Pan, B., Zhang, F., Feng, X., An, T., Marrero-Ortiz, W., Secrest, J., Zhang, A. L., Shibuya, K.,
641 Molina, M. J., and Zhang, R.: Reassessing the atmospheric oxidation mechanism of toluene,
642 Proc. Natl. Acad. Sci. U.S.A., 114, 8169-8174, 10.1073/pnas.1705463114, 2017.
643 Johnson, D., and Marston, G.: The gas-phase ozonolysis of unsaturated volatile organic
644 compounds in the troposphere, Chem. Soc. Rev., 37, 699-716, 10.1039/b704260b, 2008.
645 Kidwell, N. M., Li, H., Wang, X., Bowman, J. M., and Lester, M. I.: Unimolecular dissociation
646 dynamics of vibrationally activated CH_3CHOO Criegee intermediates to OH radical products,
647 Nat. Chem., 8, 509-514, 10.1038/NCHEM.2488, 2016.
648 Kirkby, J., Duplissy, J., Sengupta, K., Frege, C., Gordon, H., Williamson, C., Heinritzi, Martin.,
649 Simon, M., Yan, C., Almeida, J., Tröstl, J., Nieminen, T., Ortega, I. K., Wagner, R., Adamov,

A., Amorim, A., Bernhammer, A. K., Bianchi, F., Breitenlechner, M., Brilke, S., Chen, X., Craven, J., Dias, A., Ehrhart, S., Flagan, R. C., Franchin, A., Fuchs, C., Guida, R., Hakala, J., Hoyle, C. R., Jokinen, T., Junninen, H., Kangasluoma, J., Kim, J., Krapf, M., Kürten1, A., Laaksonen, A., Lehtipalo, K., Makhmutov, V., Mathot, S., Molteni, U., Onnela, A., Peräkylä, O., Piel, F., Petäjä, T., Praplan, A. P., Pringle, K., Rap, A., Richards, N. A. D., Riipinen, I., Rissanen, M. P., Rondo, L., Sarnela, N., Schobesberger, S., Scott, C. E., Seinfeld, J. H., Sipilä, M., Steiner, G., Stozhkov, Y., Stratmann, F., Tomé, A., Virtanen, A., Vogel, A. L., Wagner, A. C., Wagner, P. E., Weingartner, E., Wimmer, D., Winkler, P. M., Ye, P., Zhang, X., Hansel, A., Dommen, J., Donahue, N. M., Worsnop, D. R., Baltensperger, U., Kulmala, M., Carslaw, K. S., and Curtius, J.: Ion-induced nucleation of pure biogenic particles, Nature, 533, 521-526, 10.1038/nature17953, 2016.

Kroll, J. H., and Seinfeld, J. H.: Chemistry of secondary organic aerosol: Formation and evolution of low-volatility organics in the atmosphere, Atmos. Environ., 42, 3593-3624, 10.1016/j.atmosenv.2008.01.003, 2008.

Kroll, J. H., Clarke, J. S., Donahue, N. M., and Anderson, J. G.: Mechanism of HO_x formation in the gas-phase ozone-alkene reaction. 1. direct, pressure-dependent measurements of prompt OH yields, J. Phys. Chem. A, 105, 1554-1560, 10.1021/jp002121r, 2001.

Kroll, J. H., Sahay, S. R., and Anderson, J. G.: Mechanism of HO_x formation in the gas-phase ozone-alkene reaction. 2. prompt versus thermal dissociation of carbonyl oxides to form OH, J. Phys. Chem. A, 105, 4446-4457, 10.1021/jp004136v, 2001.

Kumar, M., Busch, D. H., Subramaniam, B., and Thompson, W. H.: Role of tunable acid catalysis in decomposition of α-hydroxyalkyl hydroperoxides and mechanistic implications for tropospheric chemistry, J. Phys. Chem. A, 118, 9701-9711, 10.1021/jp505100x, 2014.

Kumar, M., Zhong, J., Francisco, J. S., and Zeng, X. C.: Criegee intermediate-hydrogen sulfide chemistry at the air/water interface, Chem. Sci., 8, 5385-5391, 10.1039/c7sc01797a, 2017.

Kumar, M., Zhong, J., Zeng, X. C., and Francisco, J. S.: Reaction of Criegee intermediate with nitric acid at the air-water interface, J. Am. Chem. Soc., 140, 4913-4921, 10.1021/jacs.8b01191, 2018.

Kuwata, K. T., Guinn, E. J., Hermes, M. R., Fernandez, J. A., Mathison, J. M., and Huang, K.: A computational re-examination of the Criegee intermediate-sulfur dioxide reaction, J. Phys. Chem. A, 119, 10316-10335, 10.1021/acs.jpca.5b06565, 2015.

Lester, M. I., and Klippenstein, S. J.: Unimolecular decay of Criegee intermediates to OH radical products: prompt and thermal decay processes, Acc. Chem. Res., 51, 978-985, 10.1021/acs.accounts.8b00077, 2018.

Lewis, T. R., Blitz, M. A., Heard, D. E., and Seakins, P. W.: Direct evidence for a substantive reaction between the Criegee intermediate, CH_2OO, and the water vapour dimer, Phys. Chem. Chem. Phys., 17, 4859-4863, 10.1039/c4cp04750h, 2015.

Li, J., Carter, S., Bowman, J. M., Dawes, R., Xie, D., and Guo, H.: High-level, first-principles, full-dimensional quantum calculation of the ro-vibrational spectrum of the simplest criegee intermediate (CH_2OO), J. Phys. Chem. Lett., 5, 2364-2369, 10.1021/jz501059m, 2014.

Li, L., Hoffmann, M. R., and Colussi, A. J.: Role of nitrogen dioxide in the production of sulfate during Chinese haze-aerosol episodes, Environ. Sci. Technol., 52, 2686-2693, 10.1021/acs.est.7b05222, 2018.

Li, Y., Gong, Q., Yue, L., Wang, W., and Liu, F.: Photochemistry of the simplest Criegee

694 intermediate, CH_2OO: photoisomerization channel toward dioxirane revealed by CASPT2
695 calculations and trajectory surface-hopping dynamics, J. Phys. Chem. Lett., 9, 978-981,
696 10.1021/acs.jpclett.8b00023, 2018.
697 Lin, J., and Chao, W.: Structure-dependent reactivity of Criegee intermediates studied with
698 spectroscopic methods, Chem. Soc. Rev., 46, 7483-7497, 10.1039/C7CS00336F, 2017.
699 Lin, L. C., Chang, H. T., Chang, C. H., Chao, W., Smith, M. C., Chang, C. H., Lin, J. J., and
700 Takahashi, K.: Competition between H_2O and $(H_2O)_2$ reactions with CH_2OO/CH_3CHOO,
701 Phys. Chem. Chem. Phys., 18, 4557-4568, 10.1039/C5CP06446E, 2016.
702 Long, B., Bao, J. L., and Truhlar, D. G.: Atmospheric chemistry of Criegee intermediates:
703 unimolecular reactions and reactions with water, J. Am. Chem. Soc., 138, 14409-14422,
704 10.1021/jacs.6b08655, 2016.
705 Long, B., Bao, J. L., and Truhlar, D. G.: Unimolecular reaction of acetone oxide and its reaction
706 with water in the atmosphere, Proc. Natl. Acad. Sci. U.S.A., 115, 6135-6140,
707 10.1073/pnas.1804453115, 2018.
708 Mauldin, R. L., Berndt, T., Sipilä, M., Paasonen, P., Petäjä, T., Kim, S., Kurtén, T., Stratmann, F.,
709 Kerminen, V. M., and Kulmala, M.: A new atmospherically relevant oxidant of sulphur
710 dioxide, Nature, 488, 193-6, 10.1038/nature11278, 2012.
711 Nguyen, T. B., Tyndall, G. S., Crounse, J. D., Teng, A. P., Bates, K. H., Schwantes, R. H., Coggon,
712 M. M., Zhang, L., Feiner, P., Millller, D. O., Skog, K. M., Rivera-Rios, J. C., Dorris, M.,
713 Olson, K. F., Koss, A., Wild, R. J., Brown, S. S., Goldstein, A. H., Gouw, J. A., Brune, W. H.,
714 Keutsch, F. N., Seinfeld, J. H., and Wennberg, P. O.: Atmospheric fates of Criegee
715 intermediates in the ozonolysis of isoprene, Phys. Chem. Chem. Phys., 18, 10241-10254,
716 10.1039/C6CP00053C, 2016.
717 Novelli, A., Hens, K., Ernest, C. T., Martinez, M., Nölscher, A. C., Sinha, V., Paasonen, P., Petäjä,
718 T., Sipilä, M., Elste, T., Plass-Dülmer, C., Phillips, G. J., Kubistin, D., Williams, J.,
719 Vereecken, L., Lelieveld, J., and Harder, H.: Identifying Criegee intermediates as potential
720 oxidants in the troposphere, Atmos. Chem. Phys. Discuss., 10.5194/acp-2016-919, 2016.
721 Novelli, A., Hens, K., Ernest, C. T., Martinez, M., Nölscher, A. C., Sinha, V., Paasonen, P., Petäjä,
722 T., Sipilä, M., Elste, T., Plass-Dülmer, C., Phillips, G. J., Kubistin, D., Williams, J.,
723 Vereecken, L., Lelieveld, J., and Harder, H.: Estimating the atmospheric concentration of
724 Criegee intermediates and their possible interference in a FAGE-LIF instrument, Atmos.
725 Chem. Phys., 17, 7807-7826, 10.5194/acp-17-7807-2017, 2017.
726 Ouyang, B., McLeod, M. W., Jones, R. L., and Bloss, W. J.: NO_3 radical production from the
727 reaction between the Criegee intermediate CH_2OO and NO_2, Phys. Chem. Chem. Phys., 15,
728 17070-17075, 10.1039/c3cp53024h, 2013.
729 Rissanen, M. P., Kurtén,T., Sipila, M., Thornton, J. A., Kangasluoma, J., Sarnela, N., Junninen, H.,
730 Jørgensen, S., Schallhart, S., Kajos, M. K., Taipale, R., Springer, M., Mentel, T. F.,
731 Ruuskanen, T., Petäjä, T., Worsnop, D. R., Kjaergaard, H. G., and Ehn M.: The formation of
732 highly oxidized multifunctional products in the ozonolysis of cyclohexene, J. Am. Chem.
733 Soc., 136, 15596-15606, 10.1021/ja507146s, 2014.
734 Ryzhkov, A. B., and Ariya, P. A.: A theoretical study of the reactions of carbonyl oxide with water
735 in atmosphere: the role of water dimer, Chem. Phys. Lett., 367, 423-429,
736 10.1016/S0009-2614(02)01685-8, 2003.
737 Ryzhkov, A. B., and Ariya, P. A.: A theoretical study of the reactions of parent and substituted

Criegee intermediates with water and the water dimer, Phys. Chem. Chem. Phys., 6, 5042-5050, 10.1039/B408414D, 2004.

Ryzhkov, A. B., and Ariya, P. A.: The importance of water clusters $(H_2O)_n$ (n=2, ... ,4) in the reaction of Criegee intermediate with water in the atmosphere, Chem. Phys. Lett., 419, 479-485, 10.1016/j.cplett.2005.12.016, 2006.

Sadezky, A., Winterhalter, R., Kanawati, B., Römpp, A., Spengler, B., Mellouki, A., Bras, G. L., Chaimbault, P., and Moortgat, G. K.: Oligomer formation during gas-phase ozonolysis of small alkenes and enol ethers: new evidence for the central role of the Criegee intermediate as oligomer chain unit, Atmos. Chem. Phys., 8, 2667-2699, 10.5194/acp-8-2667-2008, 2008.

Sakamoto, Y., Inomata, S., and Hirokawa, J.: Oligomerization reaction of the Criegee intermediate leads to secondary organic aerosol formation in ethylene ozonolysis, J. Phys. Chem. A, 117, 12912-12921, 10.1021/jp408672m, 2013.

Shallcross, D. E., Leather, K. E., Bacak, A., Xiao, P., Lee, E. P. F., Ng, M., Mok, D. K. W., Dyke, J. M., Hossaini, R., Chipperfield, M. P., Khan, M. A. H., and Percival, C. J.: Reaction between CH_3O_2 and BrO radicals: A new source of upper troposphere lower stratosphere hydroxyl radicals, J. Phys. Chem. A, 119, 4618-4632, 10.1021/jp5108203, 2015.

Sheps, L., Scully, A. M., and Au, K.: UV absorption probing of the conformer-dependent reactivity of a Criegee intermediate CH_3CHOO, Phys. Chem. Chem. Phys., 16, 26701-26706, 10.1039/C4CP04408H, 2014.

Smith, M. C., Chang, C. H., Chao, W., Lin, L. C., Takahashi, K., Boering, K. A., and Lin, J. J. M.: Strong negative temperature dependence of the simplest Criegee intermediate CH_2OO reaction with water dimer, J. Phys. Chem. Lett., 6, 2708-2713, 10.1021/acs.jpclett.5b01109, 2015.

Stolzenburg, D., Fischer, L., Vogel, A. L., Heinritzi, M., Schervish, M., Simonc, M., Wagner, A. C., Dada, L., Ahonen, L. R., Amorim, A., Baccarini, A., Bauer, P. S., Baumgartner, B., Bergen, A., Bianchi, F., Breitenlechner, M., Brilke, S., Mazon, S. B., Chen, D., Dias, A., Draper, D. C., Duplissy, J., Haddad, I. E., Finkenzeller, H., Frege, C., Fuchs, C., Garmash, O., Gordon, H., He, X., Helm, J., Hofbauer, V., Hoyle, C. R., Kim, C., Kirkby, J., Kontkanen, J., Kürten, A., Lampilahti, J., Lawler, M., Lehtipalo, K., Leiminger, M., Mai, H., Mathot, S., Mentler, B., Molteni, U., Nie, W., Nieminen, T., Nowak, J. B., Ojdanic, A., Onnela, A., Passananti, M., Petäjä, T., Quéléver, L. L. J., Rissanen, M. P., Sarnela, N., Schallhart, S., Tauber, C., Tomé, A., Wagner, R., Wang, M., Weitz, L., Wimmer, D., Xiao, M., Yan, C., Ye, P., Zha, Q., Baltensperger, U., Curtius, J., Dommen, J., Flagan, R. C., Kulmala, M., Smith, J. N., Worsnop, D. R., Hansel, A., Donahue, N. M., and Winkler, P. M.: Rapid growth of organic aerosol nanoparticles over a wide tropospheric temperature range, Proc. Natl. Acad. Sci. U.S.A., 115, 9122-9127, 10.1073/pnas.1807604115, 2018.

Stone, D., Blitz, M., Daubney, L., Howes, N. U. M., and Seakins, P.: Kinetics of CH_2OO reactions with SO_2, NO_2, NO, H_2O and CH_3CHO as a function of pressure, Phys. Chem. Chem. Phys., 16, 1139-1149, 10.1039/c3cp54391a, 2014.

Su, Y. T., Huang, Y. H., Witek, H. A., and Lee, Y. P.: Infrared absorption spectrum of the simplest Criegee intermediate CH_2OO, Science, 340, 174-176, 10.1126/science.1234369, 2013.

Taatjes, C. A., Meloni, G., Selby, T. M., Trevitt, A. J., Osborn, D. L., Percival, C. J., and Shallcross, D. E.: Direct observation of the gas-phase criegee intermediate (CH_2OO), J. Am. Chem. Soc., 130, 11883-11885, 10.1021/ja804165q, 2008.

Taatjes, C. A., Welz, O., Eskola, A. J., Savee, J. D., Scheer, A. M., Shallcross, D. E., Rotavera, B., Lee, E. P. F., Dyke, J. M., Mok, D. K. W., Osborn, D. L., and Percival, C. J.: Direct measurements of conformer-dependent reactivity of the Criegee intermediate CH_3CHOO, Science, 340, 177-180, 10.1126/science.1234689, 2013.

Taatjes, C. A.: Criegee intermediates: what direct production and detection can teach us about reactions of carbonyl oxides, Annu. Rev. Phys. Chem., 68, 183-207, 10.1146/annurev-physchem-052516-050739, 2017.

Tobias, H. J., and Ziemann, P. J.: Kinetics of the gas-phase reactions of alcohols, aldehydes, carboxylic acids, and water with the C13 stabilized Criegee intermediate formed from ozonolysis of 1-tetradecene, J. Phys. Chem. A, 105, 6129-6135, 10.1021/jp004631r, 2001.

Tröstl, J., Chuang, W. K., Gordon, H., Heinritzi, M., Yan, C., Molteni, U., Ahlm, L., Frege, C., Bianchi, F., Wagner, R., Simon, M., Lehtipalo, K., Williamson, C., Craven, J. S., Duplissy, J., Adamov, A., Almeida, J., Bernhammer, A. K., Breitenlechner, M., Brilke, S., Dias, A., Ehrhart, S., Flagan, R. C., Franchin, A., Fuchs, C., Guida, R., Gysel, M., Hansel, A., Hoyle, C. R., Jokinen, T., Junninen, H., Kangasluoma, J., Keskinen, H., Kim, J., Krapf, M., Kürten, A., Laaksonen, A., Lawler, M., Leiminger, M., Mathot, S., Möhler, O., Nieminen, T., Onnela, A., Petäjä, T., Piel, F. M., Miettinen, P., Rissanen, M. P., Rondo, L., Sarnela, N., Schobesberger, S., Sengupta, K., Sipilä, M., Smith, J. N., Steiner, G., Tomè, A., Virtanen, A., Wagner, A. C., Weingartner, E., Wimmer, D., Winkler, P. M., Ye, P., Carslaw, K. S., Curtius, J., Dommen, J., Kirkby, J., Kulmala, M., Riipinen, I., Worsnop, D. R. Donahue, N. M., and Baltensperger, U.: The role of low-volatility organic compounds in initial particle growth in the atmosphere, Nature, 533, 527-531, 10.1038/nature18271, 2016.

Vereecken, L., Harder, H., and Novelli, A.: The reaction of Criegee intermediates with NO, RO_2, and SO_2, and their fate in the atmosphere, Phys. Chem. Chem. Phys., 14, 14682-14695, 10.1039/c2cp42300f, 2012.

Vereecken, L.: The reaction of Criegee intermediates with acids and enols, Phys. Chem. Chem. Phys., 19, 28630-28640, 10.1039/c7cp05132h, 2017.

Wang, M., Yao, L., Zheng, J., Wang, X., Chen, J., Yang, X., Worsnop, D. R., Donahue, N. M., and Wang, L.: Reactions of atmospheric particulate stabilized Criegee intermediates lead to high-molecular-weight aerosol components, Environ. Sci. Technol., 10.1021/acs.est.6b02114, 50, 5702-5710, 2016.

Welz, O., Eskola, A. J., Sheps, L., Rotavera, B., Savee, J. D., Scheer, A. M., Osborn, D. L., Lowe, D., Booth, A. M., Xiao, P., Khan, M. A. H., Percival, C. J., Shallcross, D. E., and Taatjes, C. A.: Rate coefficients of C1 and C2 Criegee intermediate reactions with formic and acetic acid near the collision limit: direct kinetics measurements and atmospheric implications, Angew. Chem. Int. Ed., 53, 4547-4550, 10.1002/anie.201400964, 2014.

Welz, O., Savee, J. D., Osborn, D. L., Subith, S. V., Percival, C. J., Shallcross, D. E., and Taatjes, C. A.: Direct kinetic measurements of Criegee intermediate (CH_2OO) formed by reaction of CH_2I with O_2, Science, 335, 204-207, 10.1126/science.1213229, 2012.

Xu, L., Kollman, M. S., Song, C., Shilling, J. E., and Ng, N. L.: Effects of NO_x on the volatility of secondary organic aerosol from isoprene photooxidation, Environ. Sci. Technol., 48, 2253-2262, 10.1021/es404842g, 2014.

Yin, C., and Takahashi, K.: How does substitution affect the unimolecular reaction rates of Criegee intermediates?, Phys. Chem. Chem. Phys., 19, 12075-12084, 10.1039/C7CP01091E,

826 2017.
827 Zhang, D., and Zhang, R.: Mechanism of OH formation from ozonolysis of isoprene: a
828 quantum-chemical study, J. Am. Chem. Soc., 124, 2692-2703, 10.1021/ja011518l, 2002.
829 Zhang, P., Wang, W. L., Zhang, T. L., Chen, L., Du, Y. M., Li, C. Y., and L ü, J.: Theoretical study
830 on the mechanism and kinetics for the self-reaction of $C_2H_5O_2$ radicals, J. Phys. Chem. A,
831 116, 4610-4620, 10.1021/jp301308u, 2012.
832 Zhang, T., Wang, R., Chen, H., Min, S., Wang, Z., Zhao, C., Xu, Q., Jin, L., Wang, W., and Wang,
833 Z.: Can a single water molecule really affect the hydrogen abstraction reaction of HO_2 + NO_2
834 under tropospheric conditions? Phys. Chem. Chem. Phys., 17, 15046-15055,
835 10.1039/C5CP00968E, 2015.
836 Zhang, W., Du, B., and Qin, Z.: Catalytic effect of water, formic acid, or sulfuric acid on the
837 reaction of formaldehyde with OH radicals, J. Phys. Chem. A, 118, 4797-4807,
838 10.1021/jp502886p, 2014.
839 Zhang, X., McVay, R. C., Huang, D. D., Dalleska, N. F., Aumont, B., Flagan, R. C., and Seinfeld,
840 J. H.: Formation and evolution of molecular products in α-pinene secondary organic aerosol,
841 Proc. Natl. Acad. Sci. U.S.A., 117, 14168-14173, 10.1073/pnas.1517742112, 2015.
842 Zhao, Q., Liu, F., Wang, W., Li, C., Lu, J., and Wang, W.: Reactions between hydroxyl-substituted
843 alkylperoxy radicals and Criegee intermediates: correlations of the electronic characteristics
844 of methyl substituents and the reactivity, Phys. Chem. Chem. Phys., 19, 15073-15083,
845 10.1039/C7CP00869D, 2017.
846 Zhao, Y., and Truhlar, D. G.: A new local density functional for main-group thermochemistry,
847 transition metal bonding, thermochemical kinetics, and noncovalent interactions, J. Chem.
848 Phys., 125, 194101-18, 10.1063/1.2370993, 2006.
849 Zhao, Y., and Truhlar, D. G.: Density functionals with broad applicability in chemistry, Acc. Chem.
850 Res., 41, 157-167, 10.1021/ar700111a, 2008.
851 Zhao, Y., and Truhlar, D. G.: The M06 suite of density functionals for main group
852 thermochemistry, thermochemical kinetics, noncovalent interactions, excited states, and
853 transition elements: two new functionals and systematic testing of four M06-class functionals
854 and 12 other functionals, Theor. Chem. Acc., 120, 215-241, 10.1007/s00214-007-0310-x,
855 2008.
856 Zhao, Y., Wingen, L. M., Perraud, V., Greaves, J., and Finlayson-Pitts, B. J.: Role of the reaction
857 of stabilized Criegee intermediates with peroxy radicals in particle formation and growth in
858 air, Phys. Chem. Chem. Phys., 17, 12500-12514, 10.1039/c5cp01171j, 2015.
859 Zheng, J., and Truhlar, D. G.: Direct dynamics study of hydrogen-transfer isomerization of
860 1-pentyl and 1-hexyl radicals, J. Phys. Chem. A, 113, 11919-11925, 10.1021/jp903345x,
861 2009.
862 Zhong, J., Kumar, M., Francisco, J. S., and Zeng, X. C.: Insight into chemistry on cloud/aerosol
863 water surfaces, Acc. Chem. Res., 51, 1229-1237, 10.1021/acs.accounts.8b00051, 2018.
864 Zhong, J., Kumar, M., Zhu, C. Q., Francisco, J. S., and Zeng, X. C.: Surprising stability of larger
865 Criegee intermediates on aqueous interfaces, Angew. Chem. Int. Ed., 56, 7740-7744,
866 10.1002/anie.201702722, 2017.
867 Zhu, C., Kumar, M., Zhong, J., Li, L., Francisco, J. S., and Zeng, X. C.: New mechanistic
868 pathways for Criegee-water chemistry at the air/water interface, J. Am. Chem. Soc., 138,
869 11164-11169, 10.1021/jacs.6b04338, 2016.

Atmos. Chem. Phys. Discuss., https://doi.org/10.5194/acp-2018-935
Manuscript under review for journal Atmos. Chem. Phys.
Discussion started: 6 November 2018

Atmospheric Chemistry and Physics Discussions

Table 1 Relative energies (kcal mol^{-1}) for the stationary points and activation energies for the elementary pathways of carbonyl oxides reactions with water dimer. Labels A, B, C, and D are defined in Figure 1

Entry	R1	R2	DO2H4O4H3	DO4H2O3H1	A	B	C	D	$\Delta E_a^{\#}$
1	H	H	-123.6	96.7	-15.2	-10.8	-49.8	-42.2	4.4
2	H	H	124.5	-94.9	-15.0	-11.0	-49.1	-42.3	4.0
3	H	H	-143.8	-116.9	-14.7	-10.6	-48.7	-42.3	4.1
4	H	H	143.0	122.7	-14.7	-9.5	-49.3	-42.4	5.2
5	CH_3	H	-126.2	100.9	-16.0	-6.6	-43.9	-36.0	9.4
6	CH_3	H	130.0	-90.4	-15.5	-6.5	-43.0	-36.3	9.0
7	CH_3	H	-146.0	-116.3	-15.8	-6.9	-42.5	-36.3	8.9
8	CH_3	H	138.1	126.3	-15.7	-5.0	-43.3	-36.0	10.2
9	H	CH_3	-122.1	95.0	-18.0	-11.2	-48.5	-40.9	6.8
10	H	CH_3	125.6	-93.6	-17.4	-11.1	-47.6	-40.9	6.3
11	H	CH_3	-138.1	-120.5	-18.0	-10.8	-46.9	-40.9	7.2
12	H	CH_3	139.2	123.4	-17.5	-9.7	-47.9	-40.9	7.8
13	CH_3	CH_3	-125.4	101.5	-18.4	-7.5	-43.0	-35.1	10.9
14	CH_3	CH_3	128.5	-89.8	-18.0	-7.1	-41.9	-35.3	10.9
15	CH_3	CH_3	-145.4	-117.6	-18.5	-7.3	-41.3	-35.3	11.2
16	CH_3	CH_3	136.3	129.4	-18.1	-5.5	-42.5	-35.1	12.6

Atmos. Chem. Phys. Discuss., https://doi.org/10.5194/acp-2018-935
Manuscript under review for journal Atmos. Chem. Phys.
Discussion started: 6 November 2018

Atmospheric Chemistry and Physics Discussions

874 **Table 2** Rate coefficients (cm^3 $molecule^{-1}$ s^{-1}) of SCIs reactions with $HO\text{-}CH_2OO\text{-}H$ computed at
875 different temperatures

T/K	k_{CH2OO}	$k_{anti\text{-}CH3CHOO}$	$k_{syn\text{-}CH3CHOO}$	$k_{(CH3)2CHOO}$
273	2.5×10^{-11}	1.4×10^{-8}	1.7×10^{-14}	6.9×10^{-12}
280	1.9×10^{-11}	9.1×10^{-9}	1.5×10^{-14}	5.7×10^{-12}
298	1.1×10^{-11}	3.4×10^{-9}	1.2×10^{-14}	3.6×10^{-12}
300	9.9×10^{-12}	3.1×10^{-9}	1.2×10^{-14}	3.4×10^{-12}
320	5.6×10^{-12}	1.2×10^{-9}	9.9×10^{-15}	2.2×10^{-12}
340	3.4×10^{-12}	5.4×10^{-10}	8.4×10^{-15}	1.5×10^{-12}
360	2.2×10^{-12}	2.6×10^{-10}	7.3×10^{-15}	1.1×10^{-12}
380	1.5×10^{-12}	1.4×10^{-10}	6.4×10^{-15}	8.2×10^{-13}
400	1.0×10^{-12}	7.7×10^{-11}	5.8×10^{-15}	6.4×10^{-13}

876

Atmos. Chem. Phys. Discuss., https://doi.org/10.5194/acp-2018-935
Manuscript under review for journal Atmos. Chem. Phys.
Discussion started: 6 November 2018

Atmospheric Chemistry and Physics Discussions

Figure Captions:

Figure 1. Schematic PES for the bimolecular reaction of SCIs with water dimer

Figure 2. PES (ΔG and ΔE (*italic*)) for the reaction of CH_2OO with HO-CH_2OO-H (Pa_1) computed at the M06-2X/def2-TZVP//M06-2X/6-311+G(2df,2p) level of theory

Figure 3. PES (ΔG and ΔE (*italic*)) for the reactions of HO-C(CH_3)HOO-H with *anti*-(a) and *syn*-CH_3CHOO(b) calculated at the M06-2X/def2-TZVP//M06-2X/6-311+G(2df,2p) level of theory

Figure 4. PES (ΔG and ΔE (*italic*)) for the reaction of $(CH_3)_2COO$ with HO-C$(CH_3)_2$OO-H(Pa_3) calculated at the M06-2X/def2-TZVP//M06-2X/6-311+G(2df,2p) level of theory

Figure 5. PES (ΔG and ΔE (*italic*)) of distinct SCI reactions with HO-CH_2OO-H calculated at the M06-2X/def2-TZVP//M06-2X/6-311+G(2df,2p) level of theory

Atmos. Chem. Phys. Discuss., https://doi.org/10.5194/acp-2018-935
Manuscript under review for journal Atmos. Chem. Phys.
Discussion started: 6 November 2018

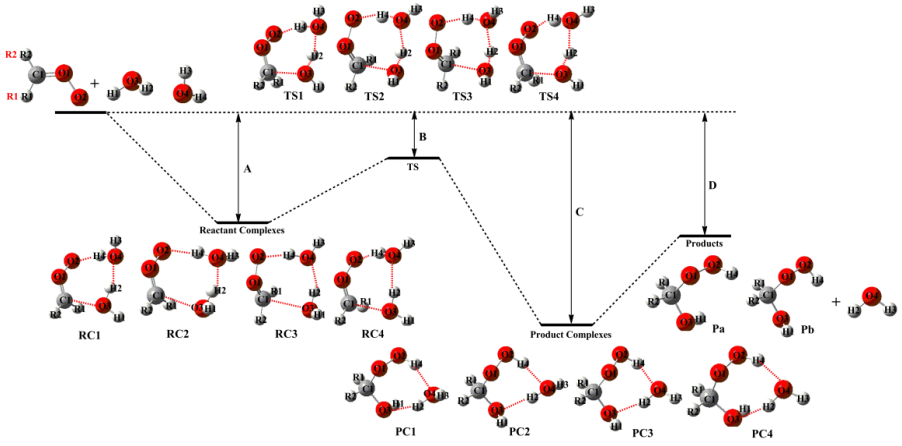

888

889 **Figure 1.**

Atmos. Chem. Phys. Discuss., https://doi.org/10.5194/acp-2018-935
Manuscript under review for journal Atmos. Chem. Phys.
Discussion started: 6 November 2018

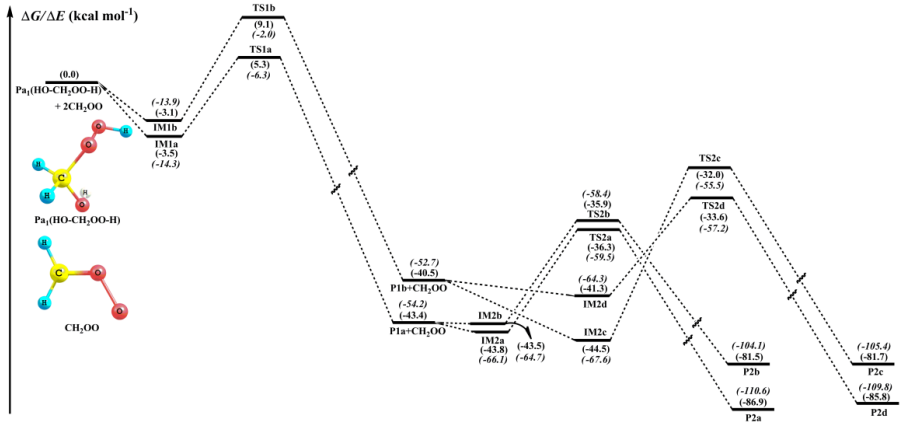

Figure 2.

Atmos. Chem. Phys. Discuss., https://doi.org/10.5194/acp-2018-935
Manuscript under review for journal Atmos. Chem. Phys.
Discussion started: 6 November 2018

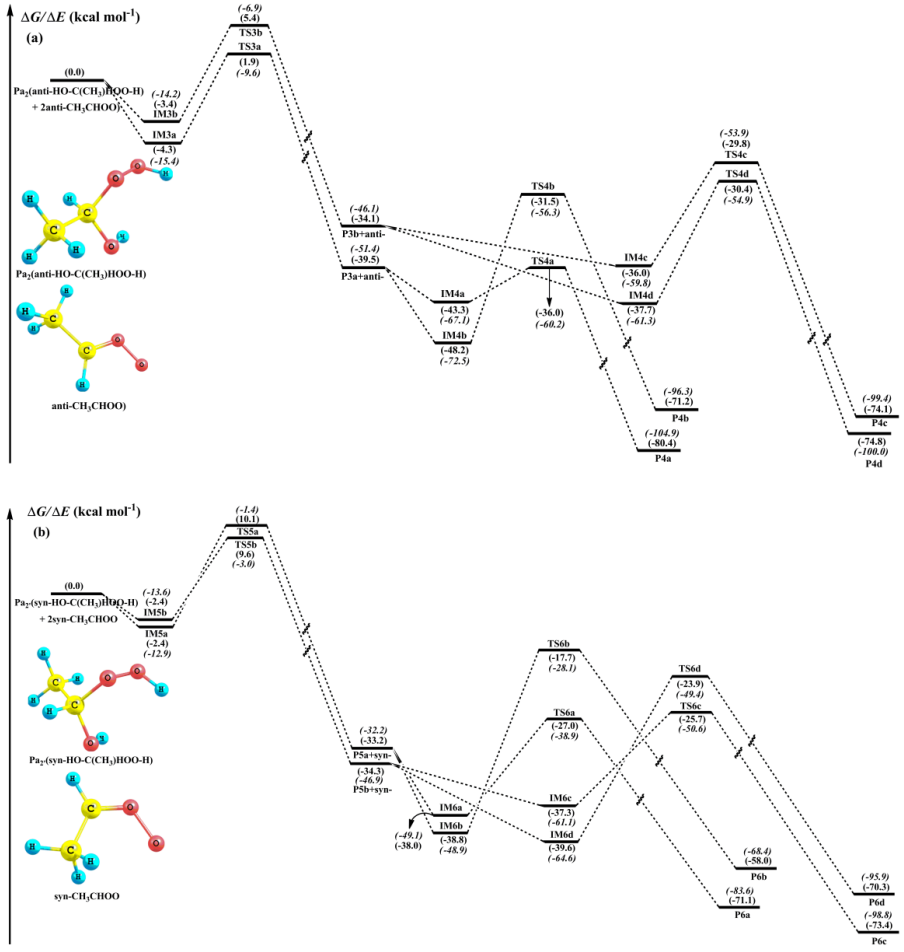

Figure 3.

Atmos. Chem. Phys. Discuss., https://doi.org/10.5194/acp-2018-935
Manuscript under review for journal Atmos. Chem. Phys.
Discussion started: 6 November 2018

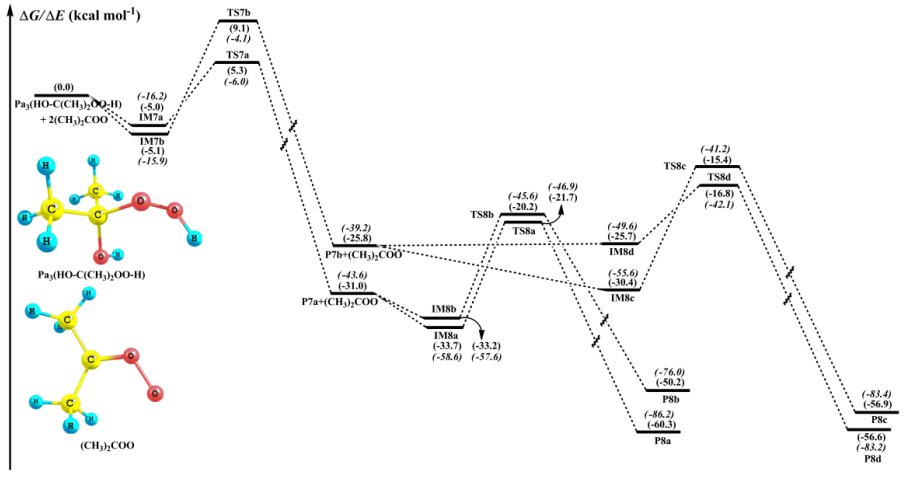

Figure 4.

Atmos. Chem. Phys. Discuss., https://doi.org/10.5194/acp-2018-935
Manuscript under review for journal Atmos. Chem. Phys.
Discussion started: 6 November 2018

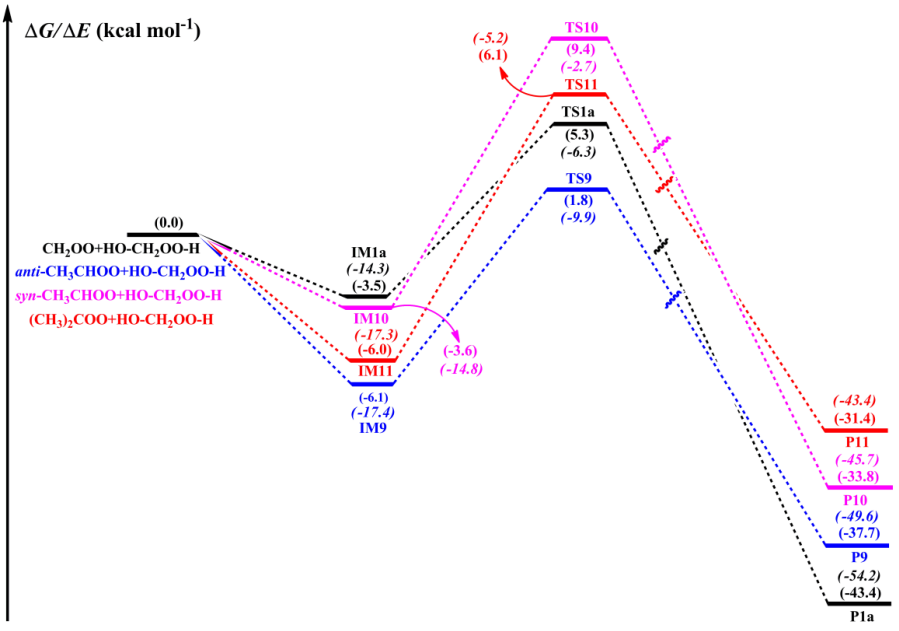

Figure 5.